Chemical Reactions in Liquids: Photolysis of OClO in Water

J. Thøgersen, C. L. Thomsen, J. Aa. Poulsen, and S. R. Keiding*,†

Department of Chemistry, University of Aarhus, Langelandsgade 140, DK-8000 Aarhus C, Denmark

Received: November 21, 1997; In Final Form: January 14, 1998

The photolysis of aqueous OClO, a key reaction in the understanding of atmospheric photochemistry, was studied using femtosecond spectroscopy. We report experimental results that resolve the current dispute over the chlorine dioxide photolysis and provide a detailed and complete example of chemical reaction dynamics in liquids. Two channels are active in the photolysis: (i) the formation of Cl atoms with a quantum yield of 0.07 ± 0.03 and (ii) the formation of ClO+O, that geminately recombine as a result of caging and forms vibrationally excited OClO, which subsequently relaxes to the vibrational ground state on a 10 ps time scale. By continuously tuning the photolysis wavelengths from 400 to 300 nm, we observe a gradual increase in the cage escape yield, as the kinetic energy of the oxygen atom becomes sufficient to break the solvent cage.

Introduction

The involvement of OClO in the photochemical processes leading to ozone depletion in the upper atmosphere[1] has served as an inspiration for numerous experimental and theoretical investigations of OClO.[2−13] Both homogeneous and heterogeneous processes are of interest due to their potential role in the atmospheric processes,[10,11] and consequently, both the gas- and condensed-phase reactivity of OClO have been considered. Recently, however, it was demonstrated that the surface concentration of OClO on ice is too low to significantly contribute to the ozone destruction in the stratosphere.[11] The gas-phase reactivity of OClO was recently studied and described by Davis and Lee[8,9] using photofragment translational spectroscopy. Davis and Lee give a detailed account of the yield of the photo products and the distribution of energy into translational and vibrational degrees of freedom. In addition they demonstrated how the yield of Cl atoms depends on the excitation wavelength, and showed how this could be explained using the potential energy surfaces calculated by Peterson and Werner.[4,5] The well-described gas-phase photolysis of OClO provides an important starting point in the interpretation of the observations in the condensed phase, to be described in this work. The photolysis of OClO in condensed phase is of great interest not only because of the atmospheric photochemistry, but also because of the current interest in elucidating the role played by the solvent, or a solid matrix, in chemical reaction dynamics. The study of the OClO photolysis in the liquid phase was pioneered by J. D. Simon and co-workers[6,7,12] and this work, as well as the gas-phase work, was recently reviewed by Vaida and Simon[2].

When aqueous OClO is photolyzed with near-ultraviolet light (400 nm) the dominant photochemical product was hitherto believed to be ClO+O, which does not cause a net removal of ozone as a result of the formation of an oxygen atom that counter-balances the ClO radical. In addition, it has been suggested[1] that formation of $Cl+O_2$ via isomerization to a long-lived ClOO isomer could contribute to the photolytic products. This reaction channel could contribute significantly to the catalytic destruction of ozone due to the presence of the Cl radical. We recently reported experimental evidence that the above model for the OClO photolysis must be adjusted.[13] In the present work we report a thorough experimental investigation that unequivocally determines the products from the near UV photolysis of OClO. This paper concludes that when aqueous OClO is photolyzed at 400 nm, $93 \pm 3\%$ of the excited molecules dissociates into ClO+O which subsequently geminately recombines to vibrationally excited OClO as a result of the solvent caging effect. Since accurate ab initio potential energy surfaces are available,[4,5] the spectral properties of vibrationally excited OClO can be calculated. The solvent induced vibrational relaxation can thus be monitored by following the time-dependent absorption of the relaxing molecules. We show below that the relaxation can be accurately described assuming that the relaxation takes place predominantly in the asymmetric stretch mode of OClO. The remaining $7 \pm 3\%$ of the excited molecules dissociates into $Cl+O_2$ within 5 ps, and these species are thus the only surviving reaction product of the 400 nm photolysis. Hence the formation of Cl does not involve a long-lived ClOO intermediate. At higher photolysis energies we observe a gradual increase in the cage escape yield, as the kinetic energy of the oxygen atoms becomes sufficient to break the solvent cage.

The spectral properties of the expected products Cl, ClO, and ClOO are known from the literature[14−17] and in combination with the calculated spectra and the experimental data they provide a precise and complete picture of the photolysis of aquaeous chlorine dioxide. All the product channels are quantitatively identified, and the ultrafast exchange of large amounts of kinetic and vibrational energy between solvent (H_2O) and solute (ClO+O and OClO) can both be observed and modeled using OClO potential energy surfaces.

Experimental Section

The experimental techniques used are described in ref 13 and only a brief description will be given here. Aqueous solutions of OClO were prepared by mixing $NaClO_2$ and $K_2S_2O_8$ (Fluka, analytical grade) with a few drops of water. The gaseous reaction products were diluted with pure nitrogen and led through 0.1 M aqueous $NaClO_2$ to remove residual Cl_2, and subsequently bubbled through three times distilled water. The

† E-mail: Keiding@kemi.aau.dk.

S1089-5639(98)00310-7 CCC: $15.00
Published on Web 04/17/1998

resulting OClO solution was stable for several weeks when kept in a dark place.

The transient absorption spectrometer is based on a kilohertz regeneratively amplified Titanium:Sapphire laser operating at 800 nm. The photolysis pulse was obtained either by doubling the fundamental (400 nm) or by quadrupling the output from a TOPAS parametric generator/amplifier (325−390 nm). The pulse energy of the quadrupled OPG/OPA output was 15−20 μJ. The photolytic products were probed with a time delayed pulse, either selected from a white light continuum (400−1024 nm), or from the doubled white light (300−400 nm), or by mixing the white light continuum with residual 400 nm light from the pump pulse (230−300 nm). Using a double beam configuration, with pulse to pulse normalization, the time and wavelength-dependent absorption of the photolysis products was obtained on a common absolute scale, with a time resolution of ∼200 fs and a detection limit for changes in the optical density of $\Delta A \sim 5 \times 10^{-5}$.

Results and Discussion

When photolyzed at 400 nm, OClO is excited from the X $^2B_1$ ground state to the $\tilde{A}$ $^2A_2$ state. In the gas-phase, depending on the excitation energy, the OClO molecule can either dissociate directly, or proceed via the almost degenerate 1^2A_1 and 1^2B_2 states, into the (ClO+O) and (Cl+O_2) product channels. The corresponding experimental results for the aqueous photolysis of OClO are summarized in Figure 1 showing a false color plot of the transient absorption spectra from 235 to 1024 nm following the photolysis pulse at 400 nm. The transient absorption is dominated by three main trends: (i) an induced bleaching around 360 nm (blue and green colors), corresponding to the removal of ground-state OClO by the photolysis pulse, (ii) an induced absorption on both sides of the bleaching (red and yellow colors), and (iii) a strong induced UV absorption the first few picoseconds for wavelengths shorter than 300 nm, indicated with white in Figure 1. We first consider the induced bleaching.

The measurements reveal that 93% of the induced bleaching recovers on a 15 ps time scale, indicating that, within 30 ps, nearly all of the OClO molecules return to the ground state as a result of geminate recombination. The rapid recovery of the induced bleaching is different from the observations in the gas phase and it suggest that the gas-phase model for the OClO photolysis must be modified in the liquid-phase. In a previous paper, we have shown that the modification in the liquid-phase is the caging of the ClO+O product channel leading to a fast recombination into ground-state OClO. Further evidence for this model can be derived from the transient absorption spectrum observed at long delays.

In Figure 2, we have shown the measured absorption spectrum obtained 40 ps after the photolysis pulse. The spectrum is obtained from a horizontal slice through the date in Figure 1 at a delay corresponding to 40 ps. The corresponding spectrum was then corrected for small bleaching caused by the remaining 7% OClO that did not return to the ground state. Also in Figure 2 we have indicated the equillibrated absorption spectra of the expected oxychlorine products, Cl, ClO, and ClOO as obtained from the literature.[14−17] The absorption spectrum of ClOO is based on the gas-phase absorption spectrum, as no data are available for ClOO in water. It should be noted that the value given in previous work[6,12,13] was too high by a factor of 2.3. It should also be noted that O and O_2 do not have significant absorption bands at the spectral range covered in the measurements. Figure 2 clearly shows that the Cl atom (and O_2) is the only product of the photolysis of OClO. The quantum yield for the formation of Cl+O_2 is measured to be 0.07 ± 0.03. In contrast to the previously proposed model,[7] we must conclude, that neither ClOO or ClO are present after the photolysis of OClO at 400 nm. Only at very short delays (τ < 2 ps) do we observe ClO, with a quantum yield of 0.93 from the ClO+O channel. However, the ClO component disappears in 1 ps as the ClO+O products recombine, and this dissociation channel is perhaps more correctly described as an asymmetrically distorted form of OClO. This process will be described in detail below. We also observe a precursor for the Cl production with a lifetime of approximately 4 ps. This could be the proposed ClOO molecules, but with a substantially shorter lifetime than the previously suggested 150 ps.[6] However, the absorption spectrum derived for this component using the kinetic model described in ref 13, differ significantly from the ground-state absorption spectrum of ClOO shown in Figure 2. We note that these conclusions are still valid when we use the corrected extinction coefficient of ClOO. The induced absorbance from the Cl precursor and the ClO molecule are seen in Figure 1 as the white and deep red regions below 300 nm. In the gas-phase, recent measurements[18] indicate that dissociation takes place in a two step process. First the molecule slowly (4.6 ps) approaches an intermediate state from where the molecule rapidly (0.25 ps) dissociates. Considering the dense manifold of vibronic states, spin−orbit, and vibronic couplings, as well as the additional degrees of freedom offered by the solvent, we thus refrain from distincly identifying the transient species observed during the first 5 ps.

Further insight into the OClO photolysis can obtained by observing the transient absorption between 400 and 1000 nm. At these wavelengths none of the expected products shows any measurable steady state absorption. Nevertheless, we observe a strong transient absorption signal extending to 1024 nm, shown as red and orange regions in Figure 1. There are two spectral and dynamical features of the visible and infrared absorption shown in Figure 3 that strongly indicates the origin of the signal. The maximum in the transient absorption shifts toward longer delays as the probe wavelength approaches the ground state OClO absorption maximum at 360 nm. In addition, the subsequent decay of the transient absorption becomes slower. At 1024 nm the decay time is 2 ps and at 439 nm the decay time has increased to more than 15 ps. These spectral characteristics are strongly indicative of a molecule undergoing vibrational relaxation. We have performed a detailed investigation of the spectral characteristics of the vibrational relaxation in OClO. This is described in ref 21. Below we will briefly describe the calculation and discuss the results and limitations of our approach.

To model this vibrational relaxation, it is necessary to know the absorption spectrum associated with vibrationally excited OClO in the electronic ground-state. A starting point for this calculation, is the expression for the cross section for a dipole allowed transition[19,20]

$$\sigma = \frac{4\pi e^2 |M^2| \omega_1}{6\hbar c} \sum_i \exp\left(\frac{-E_i}{kT}\right) \int_{-\infty}^{\infty} \langle i | i(t) \rangle \times \exp\left(\frac{iE_i t}{\hbar} + i\omega_l - \Gamma|t|\right) dt \quad (1)$$

E_i denotes the energy of the initial vibrational state, characterized by the wave function $|i\rangle$, ω_1 is the frequency of the photon, and M is the electronic transition moment. The upper state is in this formalism characterized by the time dependent evolution

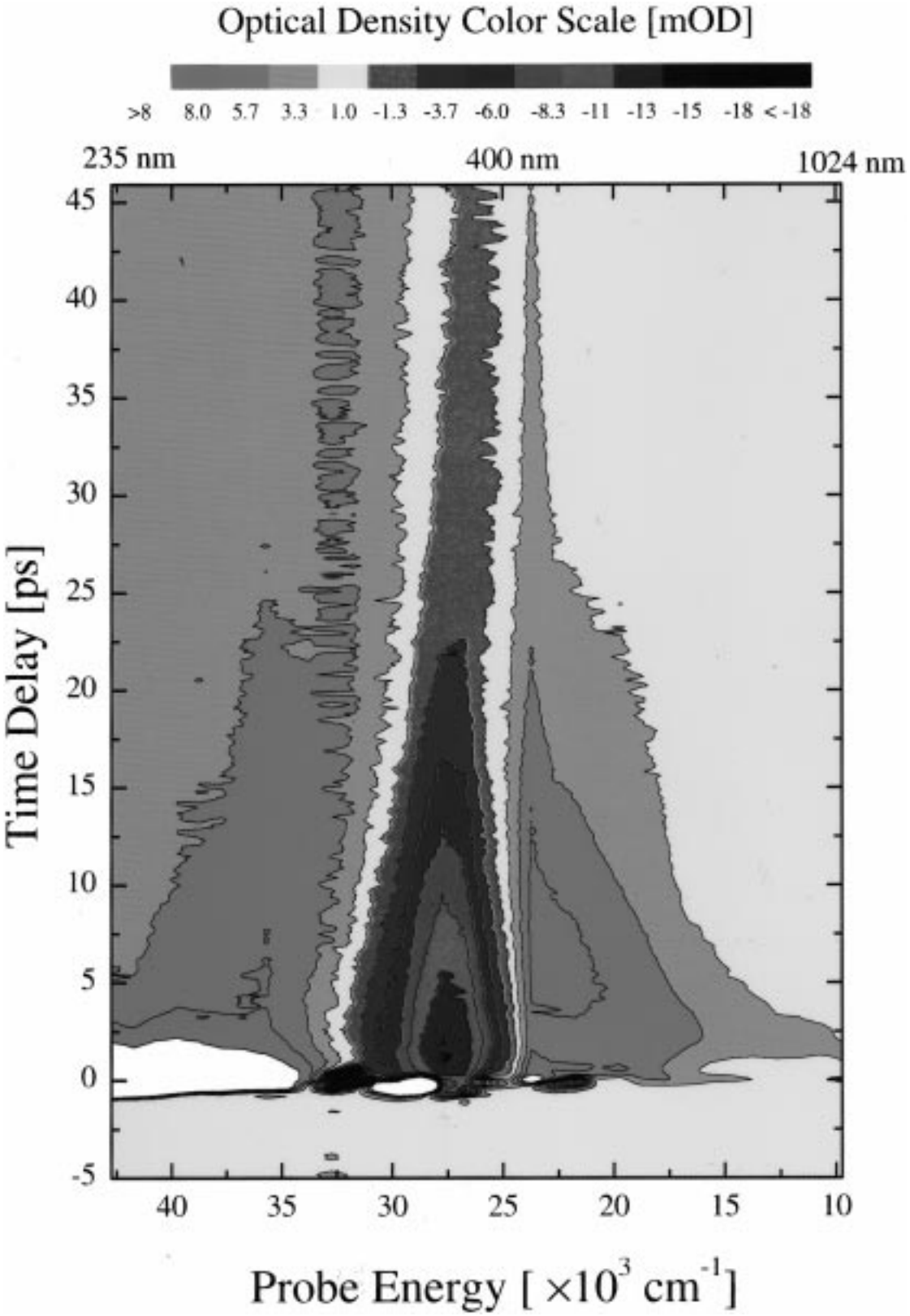

Figure 1. The transient absorption spectrum of OClO following the 400 nm photolysis pulse at $t = 0$ ps. The red and yellow colors indicated induced absorption (i.e., an increase in absorption after the photolysis pulse). After 5 ps, the induced absorption is mainly due to ground-state OClO vibrationally excited. The blue/green colors indicate an induced bleaching caused by removal of ground-state OClO. The very strong UV absorption from 370 to 240 nm at short delays is indicated with white. At 40 ps "steady state" is reached and the transient spectrum is composed only of a weak residual ground-state bleaching and the induced absorption due to the Cl radical (See Figure 2 and text).

of the initial state wave function on the upper state electronic potential energy surface $|i(t)\rangle$. Fourier transformation of the resulting time dependent Franck−Condon factors thus gives the spectral dependence of the cross section. The upper state is the $\tilde{A}\ ^2A_2$ which is obtained in refs 4 and 5. The potential surfaces are given as an expansion in the symmetry coordinates representing symmetric stretching, symmetric bending, and asymmetric stretching. No cross terms have been calculated

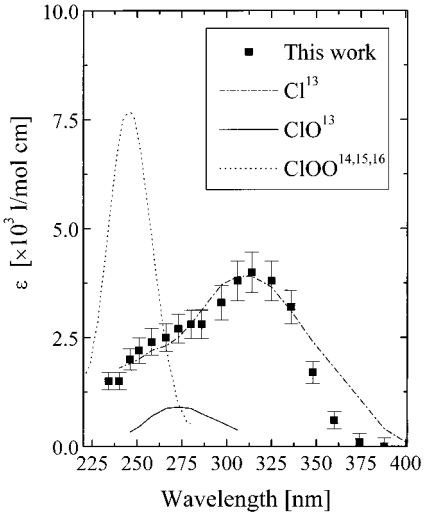

Figure 2. The steady-state absorption spectra[14−17] of the photolysis products Cl, ClOO, and ClO are shown together with the measured absorption obtained 40 ps after the photolysis pulses, corrected for the residual ground-state bleaching. There is no evidence for the formation of long-lived ClOO molecules in the photolysis.

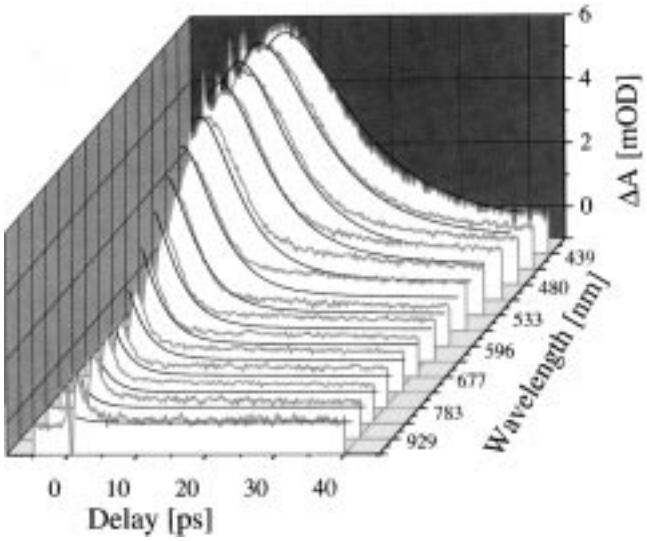

Figure 3. The time dependent induced absorption from 400 to 1024 nm. The experimental data (red lines) corresponds to absorption by the vibrationally excited OClO molecules, formed through primary geminate recombination. The transient absorption have been corrected for the very weak bleaching corresponding to the 7% of the excited OClO that forms $Cl+O_2$. The black curve is a calculation based on the potential energy surfaces calculated by Peterson and Werner[4,5] and the expression given in eq 1. Only the asymmetric stretch mode was assumed to be excited in the recombination process.

for the coupling between the symmetric modes and the asymmetric stretch, and consequently we must use the harmonic approximation for the asymmetric mode. For the symmetric modes the coupling between bending and symmetric stretch is calculated, and we can obtain the potentials to third order. We then used eq 1 to calculate the absorption spectrum for a range of both symmetric and asymmetric vibrational states in the electronic ground state. In summary, exciting the symmetric vibrations gives rise to an increased absorption both at lower and higher energies relative to the peak absorption at 362 nm. As the symmetric vibrations are excited to higher and higher states, the spectrum becomes very flat and without any structure. The asymmetric stretch, however, only gives rise to an increased absorption at lower energies relative to the OClO absorption peak. As the asymmetric stretch is excited to higher and higher states, the more the spectrum extends to the visible and near-IR. By normalizing the calculated spectrum of the vibrational ground-state to the experimental spectrum, we can also estimate the transition strength from the asymmetric vibration to be roughly twice that of the symmetric vibrations.

We can now use the calculated spectra to model the recombination process and the subsequent vibrational relaxation of the OClO molecule. In the simplest picture of the OClO photolysis we assume that the ClO+O channel is described solely by the asymmetric stretch coordinate. After excitation to the upper electronic states, the O−ClO bond is stretched until the molecule dissociates. Subsequently, the fragments collide with the solvent cage giving up all their kinetic energy. The very short lifetime observed for the ClO molecule, ($\tau \sim 1$ ps) indicates that both dissociation and recombination takes place during the first few vibrational periods. Then the O+ClO fragments begin to approach each other along the asymmetric stretch coordinate, and OClO is reformed in a highly excited vibrational state, with all of the ground-state binding energy residing in the asymmetric stretch. For the X^2B_1 ground-state the calculated binding energy is $D_0 = 2.1$ eV [4,5] (experiments[8,9,24] give $D_0 = 2.6$ eV). As a result of the solvent−solute interaction, the highly excited OClO begin to relax vibrationally. From the experimental results shown in both Figure 1 and Figure 3 we observe that the vibrational relaxation is complete in roughly 20 ps.

One can consider two extreme cases of relaxation: the vibrational relaxation can proceed either as a single-mode relaxation, where only the asymmetric stretch is excited, or as a multimode relaxation, where the two symmetric modes (stretch and bending) are being populated either as a result of solvent induced coupling between the symmetric and asymmetric modes or through internal vibrational relaxation (IVR). In the extreme case one can simply assume that the vibrational energy of the recombining fragments thermalizes very rapidly with the solvent, such that all vibrational modes are populated corresponding to a Boltzmann distribution with a temperature equivalent to the ground-state binding energy.

In Figure 3 we have shown the calculated absorption spectrum resulting from a single mode relaxation, where only the asymmetric stretch was excited and no coupling to the symmetric vibrations was assumed. The calculated spectrum assumes that roughly one-fourth of the initial 3.1 eV photolysis energy is transferred to the solvent and that all of the remaining kinetic energy (2.6 eV) is used to excited the asymmetric stretch in the OClO ground state. Thus, we start the calculation with the crude approximation, that the recombining OClO molecules, initially excited only in the asymmetric stretch, relax all the way to the lowest level without coupling to the symmetric modes. In addition we assume a simple energy dependent relaxation rate, where the relaxation time is proportional to $1/v_i$, where v_i is the asymmetric stretch vibrational quantum number. Surprisingly, even this simple model, assuming harmonic potentials, single-mode relaxation, and an energy dependent relaxation rate, is able to reproduce the experimental data very well as illustrated in Figure 3. To test the uniqueness of the agreement we have performed calculations assuming different excitation energies of the asymmetric stretch, and also excitation of purely symmetric vibrations. In all cases the agreement between calculation and observation is not as good as for the excitation into the asymmetric states at 2.6 eV. A careful comparison between the experimental data and the transient spectrum calculated from the simple kinetic model[13] and the

vibrationally relaxing OClO reveals a weak excess absorption in the UV from 7 to 20 ps. This is responsible for part of the red plamage from 300 to 250 nm in Figure 1 appearing at delays from 5 to 20 ps. We assign this excess transient absorption to OClO excited in the symmetric modes. Both the delayed appearance and the subsequent decay with a time constant similar to the decay time observed in Figure 3, supports this assignment. The most probable excitation mechanism of the symmetric modes is through a solvent mediated coupling between the asymmetric modes excited in the recombination and the symmetric bend and stretch modes. This UV absorption is discussed in more detail in ref 21.

The detailed dynamics of a geminate recombination process can be difficult to observe since the spectral response of the vibrationally excited ground-state molecule is most often not known. Considering the good agreement between the calculated and observed spectral response of the relaxing vibrationally excited OClO we can directly determine the recombination time to be faster than 0.8 ps. This indicates that the process is a primary geminate recombination process, where the fragments loose their kinetic energy upon the first collision with the surrounding solvent cage.[22] The existence of the solvent cage is the primary cause for the difference between gas-phase and liquid- (or solid-) phase reaction dynamics.

In a recent paper P. J. Reid[23] et al. studied the photolysis of OClO in both water and acetonitrile. They confirmed the observation of geminate recombination and measured a yield of 0.9 ± 0.1 in water, in good agreement with this work. In the gas-phase photolysis of OClO it has been observed [9,24] that for $\lambda \sim 400$ nm, corresponding to 3.1 eV, the mechanism for dissociation changes. For excitation energies below 3.1 eV, a barrier in the excited $\tilde{A}^2A_2$ state prevents direct dissociation to the ClO+O channel, located 2.6 eV above the ground vibrational level. Instead the $\tilde{A}^2A_2$ couples to the dissociative 1^2B_2 state via the 1^2A_1 state. The 1^2B_2 state dissociates primarily into ClO+O and a small fraction dissociates to $Cl+O_2$ (maximum yield = 3.9% at $\lambda = 404$ nm). However, if the dissociation energy exceeds 3.1 eV, the $\tilde{A}^2A_2$ barrier can be surpassed, and the OClO dissociates directly, which leads to an decrease in the Cl yield. These experimental observations are in agreement with dynamics expected from the ab initio potential energy surfaces calculated by Peterson and Werner.[4,5] Although there is considerable difference between the gas-phase and liquid-phase dynamics, we can still use the gas-phase potential curves as a guideline in the discussion of the liquid-phase reactivity. The branching between the $Cl+O_2$ channel and the ClO+O channel, at 400 nm, in different media is similar, 4% (gas),[8,9] 7% (liquid),[13,23] 7% (matrix).[25] In ref 26 a quantitative conversion of OClO into ClOO was observed. If one accounts for the contribution to the ClOO yield arising from recombination of ClO+O in the solid cage, then the primary contribution to the yield of ClOO, equivalent to the yield of Cl in gas- and liquid-phases, is roughly 7%.[26] The similar yields indicate that the primary mechanism is independent of the medium and that the strongly media-dependent product distribution is due to caging and cooling of the reaction products.

To investigate the caging dynamics further, we end this paper by reporting some preliminary measurements using a tunable photolysis pulse. Using the quadrupled TOPAS OPG/OPA system, we tuned the energy of the photolysis pulse from 3.1 to 3.8 eV, thus focusing on the region where the gas-phase dynamics changed, as a result of the barrier in the $\tilde{A}^2A_2$ state. The probe was kept at a fixed wavelength of 400 nm, where only the ground-state of OClO absorbs at long delays, as evident from Figure 2. The induced bleaching of the ground-state absorption at short delays measure the number of excited OClO molecules produced by the pump pulse. The "steady-state" bleaching observed at 40 ps measures the number of OClO that have not recombined. If we assume that the quantum yield for $Cl+O_2$ channel is independent of wavelength, not necessarily a good approximation, we can obtain the quantum yield for cage escape by taking the ratio of the induced bleaching at short and long delays. The measured quantum yield for cage escape is shown in Figure 4. From a cage escape yield of 0% at 400 nm the cage escape yield increases to ~25% at 320 nm. Interpretation of the observed cage escape is complicated by two factors: The barrier in the $\tilde{A}^2A_2$ state and unknown distribution of translational and vibrational energy among the reaction products. The $\tilde{A}^2A_2$ state barrier is at 3.1 eV relative to the vibronic ground-state of OClO and thus coincides with the onset of cage escape seen in Figure 4. The observed cage escape can thus be interpreted as a change in the dissociation mechanism allowing the molecule to dissociate directly from the $\tilde{A}^2A_2$ state above 3.1 eV. In that case we measure the $\tilde{A}^2A_2$ state barrier rather than the cage barrier. In that case we must also assume that the indirect dissociation via the 1^2A_1 and 1^2B_2 states taking place below 3.1 eV leaves the products translationally cold and vibrationally hot. Recently the OClO photolysis was investigated in acetonitrile[23] and the cage escape yield was measured to 67%. This result, together with the distribution of kinetic and vibrational energy obtained from the gas-phase measurements,[8,9] suggests that kinetic energy of the fragments increases linearly with the photolysis energy. In that case the measured cage escape yield directly probes the strength of the solvent cage. Experiments are under way to further investigate the cage escape mechanism in OClO.

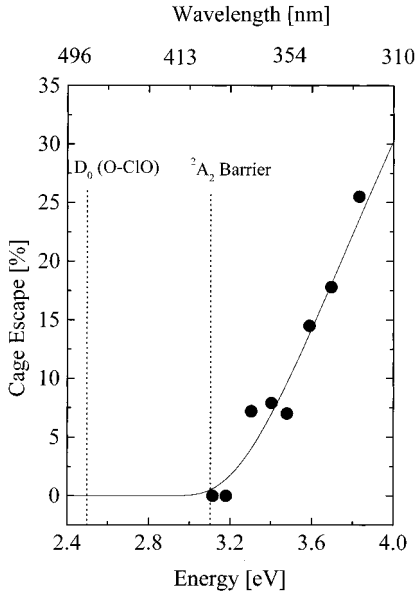

Figure 4. The ratio of cage escape to geminate recombination shown as function of the wavelength of the photolysis pulse. The uncertainty of the measured cage escape is of the order of ±5%.Also indicated in the figure is the dissociation limit of the ClO+O product channel and the barrier height of the $\tilde{A}^2A_2$ state.

Conclusions

In summary we have studied the photolysis of aqueous OClO using transient absorption spectroscopy. The transient absorption was measured from 230 to 1024 nm on a common scale with 200 fs time resolution. The only products of the photolysis

at 400 nm are Cl+O_2 with a yield of 0.07 ± 0.02. The main product channel in the gas-phase, ClO+O is closed due to caging of the fragments leading to primary geminate recombination. The subsequent formation and relaxation of hot OClO highly excited in the asymmetric stretch was observed in the transient absorption spectrum. In addition, we have modeled the transient absorption of vibrationally excited OClO using the high-level ab initio potential energy surfaces from the work of Peterson and Werner.[4,5] Excellent agreement between theory and experiment was observed if we assumed that the vibrational relaxation took place only within the asymmetric stretch mode. By tuning the photolysis wavelength, we observed a gradual increase in the percentage of ClO+O fragments, that escaped from the solvent cage. At 320 nm, corresponding to 3.8 eV, the cage escape increased to ∼25% compared to unity caging at 400 nm. We believe that the ability to tune the photolysis wavelength offers an exciting new opportunity to study the nature of the solvent cage, and thus to gain new insight into the influence of the solvent on chemical reactions in liquids.

Acknowledgment. The authors wish to acknowledge the many contributions to this work from J. R. Byberg. This work was supported by the SNF-Center for Molecular Reaction Dynamics and Laser Chemistry and the Carlsberg Foundation.

References and Notes

(1) Vaida, V.; Solomon, S.; Richards, C. E.; Ruhl, E.; Jefferson, A. *Nature* **1989**, *342*, 405.
(2) Vaida, V.; Simon, J. *Science* **1995**, *268*, 1443.
(3) Baumert, T.; Herek, J. L.; Zewail, A. H. *J. Chem. Phys*. **1993**, *99*, 4430.
(4) Peterson, K. A.; Werner, H. J. *J. Chem. Phys*. **1992**, *96*, 8948.
(5) Peterson, K. A.; Werner, H. J. *J. Chem. Phys*. **1997**, *105*, 9823.
(6) Dunn, R. C.; Simon, J. D. *J. Am. Chem. Soc*. **1992**, *114*, 4856.
(7) Chang, Y. J.; Simon, J. D. *J. Phys. Chem*. **1996**, *100*, 6406.
(8) Davis, H. F.; Lee, Y. T. *J. Phys. Chem*. **1992,** *96*, 5681.
(9) Davis, H. F.; Lee, Y. T. *J. Phys. Chem*. **1996,** *105*, 8142**.**
(10) Graham, J. D.; Roberts, J. T.; Brown, L. A.; Vaida, V. *J. Chem. Phys.* **1996**, *100*, 3115.
(11) Brown, L. A.; Vaida, V.; Hansson, D. R.; Graham, J. D.; Roberts, J. T.; *J. Chem. Phys.* **1996**, *100*, 3121.
(12) Dunn, R. C.; Flanders, B. N.; Simon, J. D. *J. Phys. Chem.* **1995**, *99*, 7360.
(13) Thøgersen, J.; Jepsen, P. U.; Thomsen, C. L.; Poulsen, J. Aa.; Byberg, J. R.; Keiding, S. R. *J. Phys. Chem. A* **1996**, *101*, 3317.
(14) Kläning, U. K.; Wolf, T. *Ber. Bunsen-Ges. Phys. Chem*. **1985**, *89*, 243.
(15) Johnston, H. S.; Morris, E. D.; Van den Bogaerde, J. *J. Am. Chem. Soc*. **1969**, *91*, 7712.
(16) Mauldin III, R. L.; Burkholder, J. B.; Ravishankara, A. R.; *J. Phys. Chem.* **1992**, *96*, 2582.
(17) Müller, H. S. P.; Willner, H. J. *J. Phys. Chem*. **1993**, *97*, 10589.
(18) Ludowise, P.; Blackwell, M.; Chen, Y. *Chem. Phys. Lett.* **1997**, *273*, 211.
(19) Kulander, K. C.; Heller, E. J. *J. Chem. Phys.* **1978**, *69*, 2439.
(20) Walhout, P. K.; Silva, C.; Barbara, P. F. *J. Phys. Chem.* **1996** *100*, 5188.
(21) Poulsen, J. Aa.; Thomsen, C. L.; Keiding, S. R.; Thøgersen, J. *J. Chem. Phys.* **1998**. In press.
(22) Schwartz, B. J.; King, J. C.; Harris, C. B. In *Ultrafast Dynamics of Chemical Systems*; Simon, J. D., Ed.; Kluwer Academic Publishers: London 1994; pp 235−248.
(23) Philpott, M. J.; Charalamabous, S.; Reid, P. J. *Chem. Phys. Lett.* **1997**.
(24) Furlan, A.; Scheld, H. A.; Huber, J. R. *J. Chem. Phys.* **1997**, *106*, 6538.
(25) Byberg, J. R. To be published.
(26) Pursell, C. J.; Conjers, J.: Alapat, P.; and Pasveen, R. *J. Phys. Chem.* **1995**, *99*, 10433.